Angular color uniformity enhancement of white light-emitting diodes by remote micro-patterned phosphor film

Shudong Yu,[1,2] Zongtao Li,[1,2,*] Guanwei Liang,[1] Yong Tang,[1] Binhai Yu,[1] and Kaihang Chen[1]

[1]*Key Laboratory of Surface Functional Structure Manufacturing of Guangdong High Education Institutes, South China University of Technology, Guangzhou 510640, China*

[2]*Optoelectronics Engineering Technology Research and Development Center, Foshan Nationstar Optoelectronics Co. Ltd., Foshan 528000, China*

**Corresponding author: ancient@yeah.net*

Received March 28, 2016; revised May 18, 2016; accepted June 12, 2016; posted June 17, 2016 (Doc. ID 262020); published July 19, 2016

Angular color uniformity (ACU) is a key factor used to evaluate the light quality of white-light emitting diodes (LEDs). In this study, a novel double remote micro-patterned phosphor film (double RMPP film) was used to enhance the ACU of a remote phosphor (RP) down-light lamp. A conventional RP film and remote phosphor film with single micro-patterned film (single RMPP film) also were examined for comparison. The angular correlated color temperature (CCT) distributions and the optical performance of the films were experimentally measured. The measurement results showed that double RMPP film configuration exhibited better color uniformity with a CCT deviation of only 441 K, compared with 556 K for the single RMPP film configuration and 1390 K for the RP film configuration. A simulation based on FDTD and ray tracing combined method also confirmed the ACU improvement. In addition, compared with the conventional RP film, the luminous efficiency of single and double RMPP film configurations was increased by 6.68% and 4.69%, respectively, at a driving current of 350 mA. The enhancement of the ACU and luminous efficiency are due to the scattering and mixing effect of the micro-patterned film. Moreover, the double RMPP film configuration had better CCT stability at different currents than the other two configurations. The results demonstrated the effectiveness and superiority of double RMPP film in white LED applications.

OCIS codes: (230.3670) Light-emitting diodes; (220.4000) Microstructure fabrication; (160.2540) Fluorescent and luminescent materials; (290.0290) Scattering.

http://dx.doi.org/10.1364/PRJ.4.000140

1. INTRODUCTION

The Nobel Prize in Physics 2014 was awarded jointly to Isamu Akasaki, Hiroshi Amano, and Shuji Nakamura for the invention of efficient blue-light emitting diodes (LEDs), which has enabled bright and energy-saving white-light sources. Nowadays, white-LEDs are increasingly becoming part of our daily life in many areas, such as general lighting, medical, and lifestyle products [1]. The most common method to generate white light is to combine blue light emitted by the LED chip and re-emission by downconverted phosphor, known as phosphor-converted LEDs (pcLEDs). Various phosphor coating methods have been proposed to obtain pcLEDs, such as dispensing and conformal coating. However, the above coating methods suffer from low luminous efficiency due to the severe absorption of backscattered light by the LED chip [2,3]. The remote phosphor (RP) configuration, in which the phosphor layer is separated from the chip, was proposed to enhance luminous efficiency by reducing phosphor emission reflection back into the LED chip [4,5]. Moreover, the RP configuration can improve the reliability of white LEDs because the backscattered light is seldom absorbed by the LED chip, and the junction temperature can thus be reduced [6]. Recent years have witnessed the great development of RP LEDs, especially in luminous efficiency enhancement. In 2011, Philips won the L Prize set by the U.S. Department of Energy for coming up with an RP lamp that is equivalent to a standard 60 W incandescent bulb in size and brightness but lasts at least 25 times as long and runs on less than 10 W. Intermatix has developed superior RP technology, known as "ChromaLit," to deliver luminous efficacy gains of up to 30% compared with a conventional LED lighting system. Furthermore, a series of RP products also are available, such as ChromaLit, ChromaLit XT, and so on. Due to its high efficiency, the RP configuration also has been utilized in quantum dot LEDs to improve their light emission and heat dissipation ability [7]. Although high in luminous efficiency, RP LEDs still suffer from poor angular color uniformity (ACU), especially for planar RP configurations [8–10]. Generally, a diffusing sheet is used to obtain uniform correlated color temperature (CCT) distribution and illumination; however, it causes energy loss during light transmission through the film [11–14]. In addition, Kuo *et al.* [15] proposed a patterned RP coating to improve the uniformity of an angular-dependent CCT, which exhibited 1.12% light loss at a driving current of 150 mA. Wang *et al.* [16] utilized a free-form lens to overlap light with different radiation angles, thus eliminating the yellow ring phenomenon. Multilayer phosphor-in-glass structure was proposed by Wang *et al.* [17] to improve ACU of LED packages with the sacrifice of luminous loss. Li *et al.* [18] also demonstrated a multilayer structure with excellent color uniformity. However, the above methods achieve

high ACU at the expense of light efficiency. Other structures, such as the patterned sapphire substrate (PSS) [19], the DBR structure [20], and the light-recycling dichroic filter [21], also were developed to enhance ACU; however, the devices have high cost and are not easy to combine with existing lighting systems. To provide a low-cost, easily integrated solution with high ACU and luminous efficiency, we introduce a remote micro-patterned phosphor (RMPP) film to replace the conventional planar RP plate in white LEDs. The RMPP film is composed of a multilayer structure in which planar RP layer is sandwiched between micro-patterned (MP) polydimethylsiloxane (PDMS) films. The optical characteristics of the MP film were measured and compared. The angle-dependent CCT distribution was evaluated for three different RP configurations whose optical performance was measured with the driving current ranging from 100 to 1000 mA. The related experimental results and analysis are illustrated.

2. EXPERIMENTS AND MEASUREMENT

In this study, an RMPP film with uniform thickness was fabricated by the spin-coating method for simplicity. Other highly efficient methods such as slot-die coating have been proposed to fabricate RP film; this method also is suitable for the RMPP film fabrication in this work [13]. A PSS was utilized as the template to obtain an MP film with a micro-concave array. The process is illustrated in Fig. 1. First, a mixture of PDMS (Dow Corning Sylgard-184) and the cross-linking agent was prepared with the mass ratio of 10:1. Then, 1 mL liquid of PDMS was dispensed on the PSS. After a 1 min spin-coating process, solidification was performed in an oven of 150°C for 1 h. Similarly, a YAG phosphor (YAG04 from Intematix) PDMS mixture with a mass ratio of 1.6:2 was prepared. The same process was conducted to form a uniform RP film. Finally, another MP film was applied on the phosphor layer to obtain a double RMPP film. An RP film with a single MP film was used for comparison, namely, single RMPP film. Due to the scattering and diffraction effect of the micro-concave array, the MP film, which has a thickness uniformity of 97.83%, exhibits rainbow colors in daylight, as shown in Fig. 2(a). The RMPP film is sufficiently flexible to allow its easy integration in various LED lighting systems. As shown in Fig. 2(b), the MP film achieves a highly accurate complementary replication of the micro-convex array on the PSS. Figures 2(c) and 2(d) show that the phosphor and the PDMS layer have a thickness of 125 and 120 μm, respectively. The small thickness difference is due to the increasing viscosity of the PDMS mixture with the addition of phosphor powder. The micro-concave has an apex angle of 90° and a height of 1.3 μm, and the distance of two adjacent micro-concaves is 3 μm. The MP film, which is positioned upward with the micro-concave array facing the light source, is named as upward-facing MP film (UF-MP film). The other configuration is called the downward-facing MP film (DF-MP film).

To verify the effectiveness of the proposed RMPP film, a remote down-light lamp was designed and fabricated. As shown in Fig. 3(a), the remote lamp was composed of three parts: an aluminous lamp body, a blue LED component, and an RP film. The lamp body was composed of a lamp base and a cylindrical reflector with a highly reflective chrome plating. A blue 3535-LED component (Foshan Nationstar) was fitted tightly on the surface of lamp base, which served as a heat sink. In addition, the relative position between the base and the reflector is adjusted to form a viewing angle of 120°. Moreover, different types of RP film covered the top surface of the lamp, acting as blue-light converter. The transmittance, reflectance, and haze properties of MP film were measured by an ultraviolet-visible spectrophotometer (Shimadzu UV-2600). The angle-dependent CCT distribution and luminous intensity were measured by a homemade instrument equipped with an Ocean Optics spectrometer positioned at a distance of 316 mm (CIE test method condition A). The luminous flux was measured in a 0.5 m diameter integrating sphere (Otsuka LE5400) at a driving current range from 100 to 1000 mA with 50 mA step. The lamp was powered by a Keithley 2450 DC source. Also, three different emission spectra were obtained at 350 mA and compared. The CCT also was obtained at different driving currents to demonstrate the color stability of the lamp covered with the RMPP film. The uncertainties of CCT, luminous intensity, and luminous flux are 0.14%, 0.18%, and 0.58%, respectively.

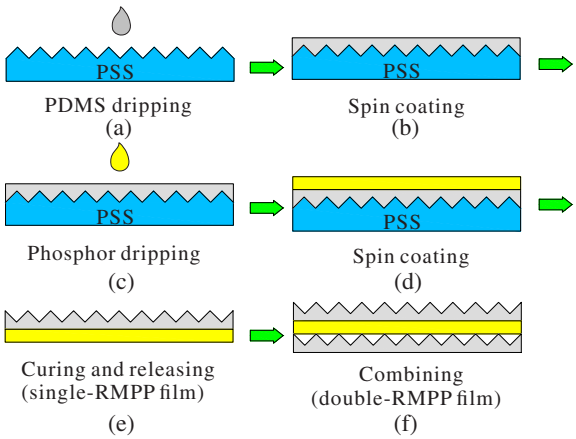

Fig. 1. Manufacturing process of RMPP film.

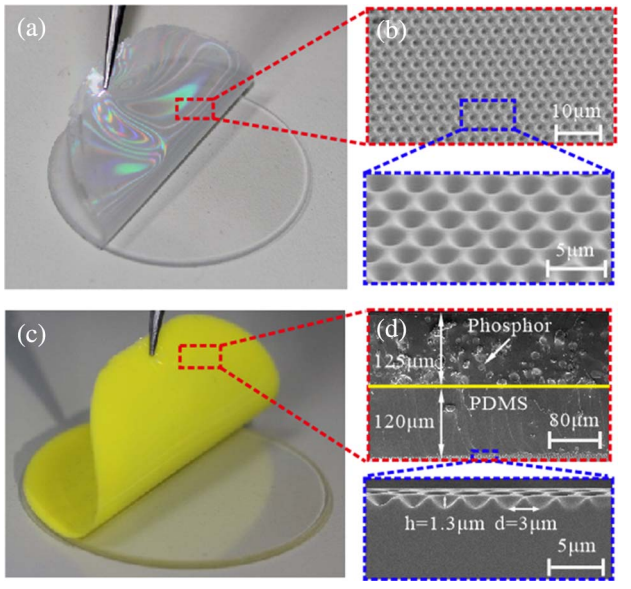

Fig. 2. (a) Photograph of MP film. (b) SEM image of its microstructure. (c) Photograph of RMPP film and (d) its cross-section SEM image.

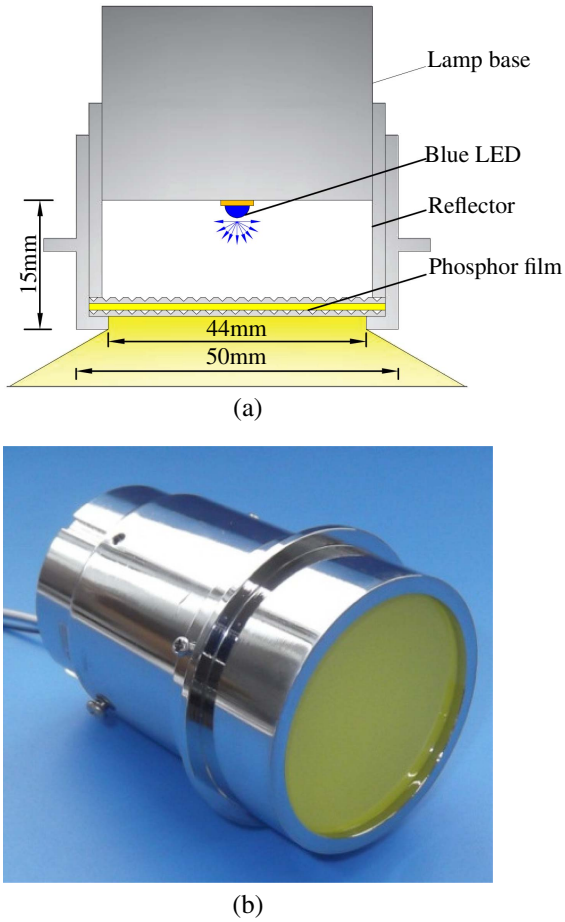

Fig. 3. (a) Schematic cross-sectional view. (b) Photograph of remote down-light lamp.

3. RESULTS AND DISCUSSION

Figure 4 shows the measured optical characteristics of the UF-MP and DF-MP films in the visible light range of 380–780 nm. As shown in Fig. 4(a), the average transmittance of the UF-MP and DF-MP film is 95% and 76%, while the average reflectance is 5% and 20%, respectively. The transmittance of the UF-MP film is 19% higher and its reflectance is 15% lower than those of the DF-MP film. The calculated absorptions of the UF-MP and DF-MP film are 0% and 6%, respectively. Reflection appears on the PDMS/air interface and the micro-concave surface causes more reflection than the flat surface. Therefore, the DF-MP film has higher reflectance than the UF-MP film. Owning to the total internal reflection at the PDMS/air interface, the light reflected by the micro-concave array is partly trapped in the PDMS layer of DF-MP film, which brings more light energy loss. When the micro-concave structure is positioned upward, direct reflection is greatly reduced because no total internal refection occurs when light is transmitted from a thinner medium (air: $n \approx 1$) to a denser one (PDMS: $n \approx 1.41$). Thus, the UF-MP film exhibits higher transmittance and lower reflectance than the DF-MP film.

As shown in Fig. 4(b), the average haze values of the UF-MP and DF-MP film are 84% and 78%, respectively; the haze value of the UF-MP film is 6% higher than that of the DF-MP film. The inset in Fig. 4(b) illustrates that the UF-MP film has a narrower scattering field distribution than the DF-MP film.

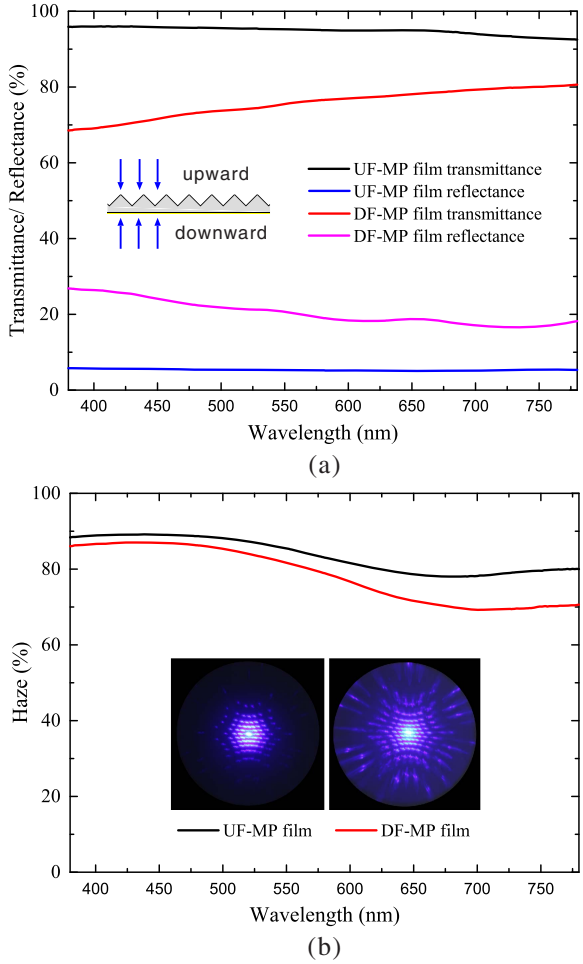

Fig. 4. (a) Wavelength-dependent transmittance and reflectance. (b) Haze of the UF-MP film and DF-MP film. Inset: photographs of light spot of the UF-MP film and DF-MP film.

This difference is attributed to two main reasons. First, total internal reflection (critical angle ≈45°) occurred at the PDMS/air interface for the UF-MP film, which limited the extraction of large-angle rays. Second, the refractive angle in the air increased when light was transmitted from the PDMS to air.

The above measurement results illustrate that the UF-MP film shows higher transmittance and more light scattering toward the peripheral region. Therefore, the UF-MP film is more suitable for the fabrication of the RMPP film.

Figure 5 displays the angle-dependent CCT distributions from −80° to 80° and the illumination patterns of three different configurations. As shown in Figs. 5(a)–5(c), the RP film configuration shows a severe yellow ring phenomenon, caused by the low intensity of the blue light at large viewing angles; in contrast, the yellow ring is greatly reduced in the RMPP configuration, especially in the lamp with the double RMPP film. In Fig. 5(d), the CCT distribution of the RP configuration shows great fluctuation, whereas those of the RMPP configurations are more flat, which means that the ACU of the latter is better than that of the former. As a counterpart of the RP film configuration, the CCT of the single RMPP film configuration exhibits drop from 8612 to 6026 K in the normal direction and a decrease from 4463 to 4398 K at a viewing angle

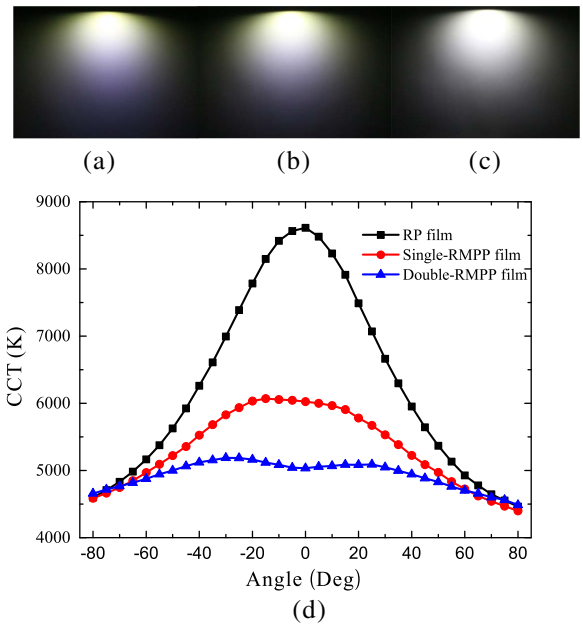

Fig. 5. (a)–(c) Illumination patterns and (d) angular CCT distributions of white LEDs with RP film, single RMPP film, and double RMPP film.

of 80°. Furthermore, the central CCT of the double RMPP film configuration is reduced from 6026 to 5034 K and its peripheral CCT level increases from 4398 to 4485 K compared with that of the single RMPP film configuration. The standard angular CCT deviations of these three configurations are 1390 K, 556 K, and 441 K, respectively. The scattering characteristics and mixing effect of the micro-concave array are the main causes of the ACU improvement.

In the single RMPP configuration, the UF-MP film can scatter the blue light from the center to the peripheral region, hence lowering the central intensity and improving the peripheral one; this result is demonstrated in Fig. 6. In Fig. 6(a), the intensity distribution of the no-film configuration is similar to that of a Lambertian source, and the deviation at large viewing angles might be caused by the absorption of the lamp reflector. By adding the MP film, the central intensity of the UF-MP film decreases from 0.99 to 0.72, while the peripheral intensity exhibits a small increase, especially at large viewing angles. Owing to the decrease of the central blue-light intensity, less yellow light is emitted and the central yellow–blue ratio (YBR) drops. The decrease of the CCT value at large viewing angles could be attributed to the re-utilization of the backscattered blue light owing to the high reflectance of the micro-concave array and lamp reflector. Consequently, more blue light is converted into yellow light, and a lower CCT is achieved at large viewing angles.

In the double-RMPP film configuration, the further increase of the ACU is due to the mixing effect of rays with different CCT values. The central light, which has high CCT, is scattered toward the peripheral region, and the large-angle light is scattered toward the central region, thus mixing together to form a more uniform viewing field. Owing to the near-Lambertian distribution, the central intensity is higher than the peripheral one. Therefore, the central light is more sensitive to the mixing effect of rays with lower CCT and exhibits a CCT level similar to that of the peripheral region.

Simulation results also verified the CCT reduction. The simulations were based on the FDTD and ray-tracing combined method (details have been described in our previously published papers [22,23]). In Fig. 6, the central YBR value of 0.43 shows significant increase to 0.47 and 0.68 for the single and double RMPP film, respectively. Considering that a lower YBR value indicates higher CCT, the simulation results are in good agreement with the experimental measurement. Here, we defined the ACU as the ratio of the minimum YBR value to the maximum one. The ACU values in the simulation were 0.38, 0.66, and 0.91 for RP, single RMPP, and double RMPP film configurations, and the increase ratios are 74% and 139%, respectively.

To further understand the optical performance of the three types of RP film, the current-dependent luminous flux was measured, and the luminous efficiency was calculated. As shown in Fig. 7(a), the luminous efficiencies of the single and double RMPP film configurations increase by 6.68% and 4.69%, respectively, at a driving current of 350 mA. This increase is attributed to the enhancement of the phosphor excitation, which is demonstrated in Fig. 7(b). In Fig. 7(b), the peak blue emissions are reduced by 12.86% and 24.99%, whereas the peak yellow-emission emissions increase by 6.95% and 4.69% for the single RMPP and double RMPP film, respectively. Because human eyes are more sensitive to yellow than to blue

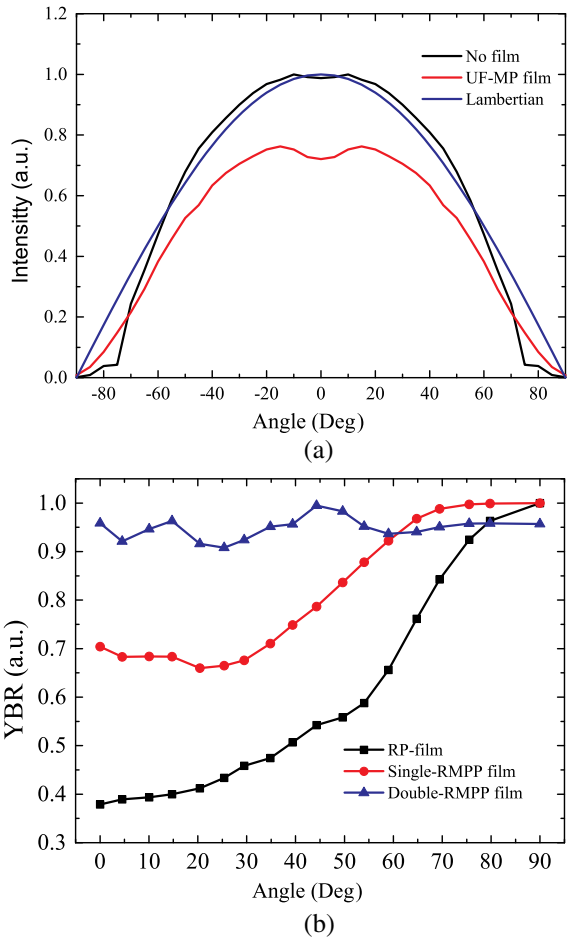

Fig. 6. (a) Normalized intensity of blue LED chip with and without the MP PDMS film. (b) YBR distributions of white LEDs with RP film, single RMPP film, and double RMPP film.

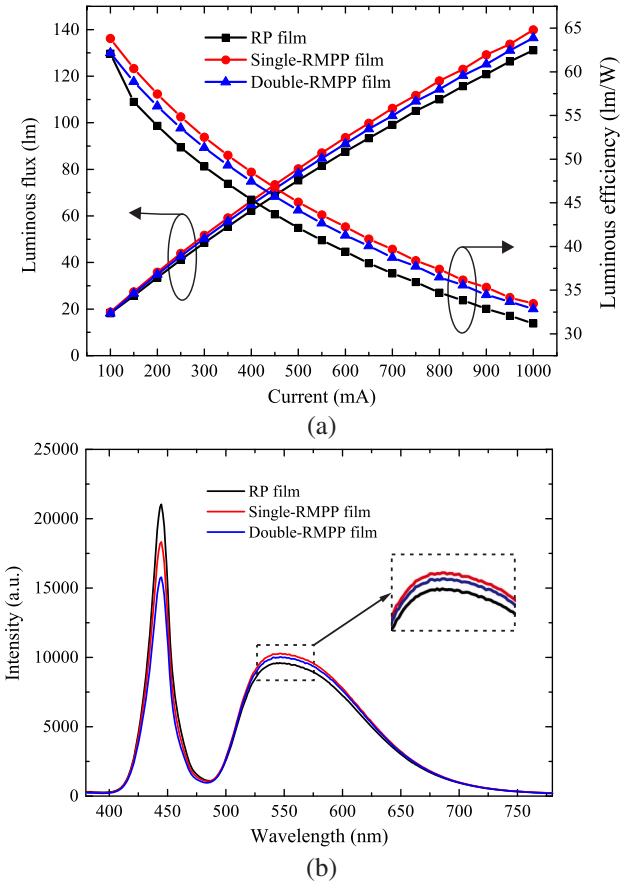

Fig. 7. (a) Luminous flux and luminous efficiency. (b) Emission spectrum of white LEDs with RP film, single RMPP film, and double RMPP film.

light, the total flux of the lamp with the RMPP film increases. With the single MP film, the CCT of the RP lamp drops from 6163 to 5537 K at a driving current of 350 mA. A lower CCT than that of the traditional configuration is achieved, and the phosphor mass could be reduced for the RMPP film under the same CCT.

For the single RMPP film, the higher phosphor excitation is due to the broader blue-light emission and the re-utilization of backscattered light. The original blue-light emission is similar to the Lambertian distribution and has lower excitation efficiency than the single RMPP film configuration, especially at large viewing angles. When the MP film is added, the central light is scattered toward the peripheral region, thus improving the relative intensity at large viewing angles. Therefore, more yellow light is produced and extracted. To our knowledge, more than half of the light scattered by the phosphor is transmitted backward [5]. The high reflectance of the micro-concave array can re-direct the backward-scattered light to the forward direction, and the light transmitted into the lamp could be reflected by the reflector; then, the MP film functions again to scatter the reflected light. The repetition of this process eventually causes the generation of even more yellow light.

Compared with the single RMPP film configuration, the double RMPP film configuration achieves better ACU at the expense of luminous efficiency. The decrease in luminous efficiency for the double configuration is due to the air gap

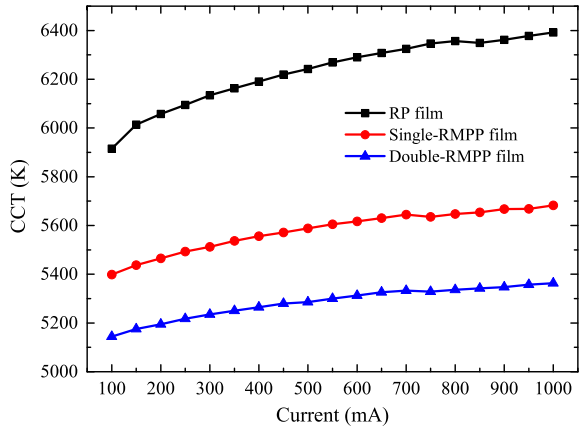

Fig. 8. Current-dependent CCT distributions for the RP film, single RMPP film, and double RMPP film configuration.

between the phosphor layer and the upper MP film [24]. The light extracted from the phosphor layer is partially trapped in the air gap because of the total internal reflection at the interface, and the emission power from 380 to 780 nm is drastically reduced. In addition, the trapped light in the air gap increases the emission of yellow phosphor; thus, the CCT is reduced from 5537 to 5250 K (350 mA), and the phosphor utilization is further improved. The luminous efficiency decrease is in a reasonable range when the upper MP film is added. Actually, the double configuration still exhibits a luminous efficiency improvement of 4.69% compared with the conventional RP film. Therefore, the proposed double RMPP film is effective in achieving high ACU in the RP lamp and an improvement in luminous efficiency.

To investigate the CCT stability of the three configurations, the current-dependent CCT was measured from 100 to 1000 mA, as shown in Fig. 8. When the driving current increases, more blue photons are generated from the LED chip, and more yellow light is downconverted. Owing to the lower excitation efficiency at larger currents, the CCT increases. For WLEDs, the method of phosphor utilization determines the color mixing quality [25]. When the driving current ranges from 100 to 1000 mA, the CCT deviations of the double and single RMPP film configurations decrease by 54.1% and 40.5%, respectively. The reduced CCT deviation is attributed to the higher utilization of phosphor for the double RMPP film, which maintains almost the same CCT at different currents. The double RMPP film not only achieves better ACU but also exhibits better CCT stability.

4. CONCLUSION

In this work, a double RMPP film was used to enhance the ACU of an RP down-light lamp. An MP film was fabricated by spin coating and was combined with an RP film on both sides. The measurement results revealed higher transmission and better scattering ability of UF-MP film, which was suitable for combination with the RP film. The results showed that the double RMPP film configuration exhibited better color uniformity with a CCT deviation of only 441 K, compared with 556 K observed for the single RMPP film configuration and 1390 K for the RP film configuration. This result was confirmed by the FDTD and ray tracing combined simulation. Compared with conventional RP film, the luminous efficiency

of the single and the double RMPP film configuration was increased by 6.68% and 4.69% at a driving current of 350 mA, respectively. When the driving current changed from 100 to 1000 mA, the CCT deviations of double RMPP film and single RMPP film configurations decreased by 54.1% and 40.5%, respectively. This decrease is attributed to the scattering and mixing effect of the MP film, which not only matches well the blue and yellow emissions to generate better color uniformity but also enhances the phosphor utilization to obtain higher flux and stable CCT. Therefore, the introduction of double RMPP film into the RP lamp is an effective and promising solution in WLEDs.

Funding. National Natural Science Foundation of China (NSFC) (U1401249, 51405161); Guandong Natural Science Foundation (2014A030312017); China Postdoctoral Science Foundation (2015T80904); Science & Technology Program of Guangdong Province (2014B010121002).

Acknowledgment. The authors would like to acknowledge useful advice by Jiasheng Li, Qiu Chen, and Xinrui Ding and the good care from Miss Fang Dong.

REFERENCES

1. P. Pust, P. J. Schmidt, and W. Schnick, "A revolution in lighting," Nat. Mater. **14**, 454–458 (2015).
2. H.-T. Huang, C.-C. Tsai, and Y.-P. Huang, "Conformal phosphor coating using pulsed spray to reduce color deviation of white LEDs," Opt. Express **18**, A201–A206 (2010).
3. R. Hu, X. Luo, and S. Liu, "Study on the optical properties of conformal coating light-emitting diode by Monte Carlo simulation," IEEE Photon. Technol. Lett. **23**, 1673–1675 (2011).
4. N. Narendran, Y. Gu, J. Freyssinier-Nova, and Y. Zhu, "Extracting phosphor-scattered photons to improve white LED efficiency," Phys. Status Solidi A **202**, R60–R62 (2005).
5. S. C. Allen and A. J. Steckl, "ELiXIR-solid-state luminaire with enhanced light extraction by internal reflection," J. Disp. Technol. **3**, 155–159 (2007).
6. K. J. Chen, B. C. Lin, H. C. Chen, M. H. Shih, C. H. Wang, H. T. Kuo, H. H. Tsai, M. Y. Kuo, S. H. Chien, P. T. Lee, C. C. Lin, and H. C. Kuo, "Effect of the thermal characteristics of phosphor for the conformal and remote structures in white light-emitting diodes," IEEE Photon. J. **5**, 8200508 (2013).
7. B. Xie, R. Hu, X. Yu, B. Shang, Y. Ma, and X. Luo, "Effect of packaging method on performance of light-emitting diodes with quantum dot phosphor," IEEE Photon. Technol. Lett. **28**, 1115–1118 (2016).
8. Z. Liu, S. Liu, K. Wang, and X. Luo, "Optical analysis of color distribution in white LEDs with various packaging methods," IEEE Photon. Technol. Lett. **20**, 2027–2029 (2008).
9. L. Xiang, Z. Huai, G. Xing, C. Jingcao, L. Sheng, and L. Peizhao, "Optical performance enhancement of quantum dot-based light-emitting diodes through an optimized remote structure," IEEE Trans. Electron Devices **63**, 691–697 (2016).
10. S. P. Ying and H. Y. Chien, "Effect of reassembled remote phosphor geometry on the luminous efficiency and spectra of white light-emitting diodes with excellent color rendering property," IEEE Trans. Electron Devices **63**, 1117–1121 (2016).
11. C. Hoelen, H. Borel, J. de Graaf, M. Keuper, M. Lankhorst, C. Mutter, L. Waumans, and R. Wegh, "Remote phosphor LED modules for general illumination: toward 200 lm/W general lighting LED light sources," Proc. SPIE **7058**, 70580M (2008).
12. H.-T. Huang, C.-C. Tsai, and Y.-P. Huang, "A direct-view backlight with UV excited trichromatic phosphor conversion film," J. Disp. Technol. **6**, 128–134 (2010).
13. H.-T. Huang, Y.-P. Huang, and C.-C. Tsai, "Planar lighting system using array of blue LEDs to excite yellow remote phosphor film," J. Disp. Technol. **7**, 44–51 (2011).
14. H. Xiao, Y.-J. Lu, T.-M. Shih, L.-H. Zhu, S.-Q. Lin, P. J. Pagni, and Z. Chen, "Improvements on remote diffuser-phosphor-packaged light-emitting diode systems," IEEE Photon. J. **6**, 1–8 (2014).
15. H.-C. Kuo, C.-W. Hung, H.-C. Chen, K.-J. Chen, C.-H. Wang, C.-W. Sher, C.-C. Yeh, C.-C. Lin, C.-H. Chen, and Y.-J. Cheng, "Patterned structure of remote phosphor for phosphor-converted white LEDs," Opt. Express **19**, A930–A936 (2011).
16. K. Wang, D. Wu, F. Chen, Z. Liu, X. Luo, and S. Liu, "Angular color uniformity enhancement of white light-emitting diodes integrated with freeform lenses," Opt. Lett. **35**, 1860–1862 (2010).
17. S. Wang, X. Chen, M. Chen, H. Zheng, H. Yang, and S. Liu, "Improvement in angular color uniformity of white light-emitting diodes using screen-printed multilayer phosphor-in-glass," Appl. Opt. **53**, 8492–8498 (2014).
18. Z.-T. Li, Y. Tang, Z.-Y. Liu, Y.-E. Tan, and B.-M. Zhu, "Detailed study on pulse-sprayed conformal phosphor configurations for LEDs," J. Disp. Technol. **9**, 433–440 (2013).
19. K.-C. Huang, T.-H. Lai, and C.-Y. Chen, "Improved CCT uniformity of white LED using remote phosphor with patterned sapphire substrate," Appl. Opt. **52**, 7376–7381 (2013).
20. H.-Y. Lin, K.-J. Chen, S.-W. Wang, C.-C. Lin, K.-Y. Wang, J.-R. Li, P.-T. Lee, M.-H. Shih, X. Li, and H.-M. Chen, "Improvement of light quality by DBR structure in white LED," Opt. Express **23**, A27–A33 (2015).
21. J. H. Oh, S. J. Yang, and Y. Rag, "Polarized white light from LEDs using remote-phosphor layer sandwiched between reflective polarizer and light-recycling dichroic filter," Opt. Express **21**, A765–A773 (2013).
22. X. Ding, J. Li, Q. Chen, Y. Tang, Z. Li, and B. Yu, "Improving LED CCT uniformity using micropatterned films optimized by combining ray tracing and FDTD methods," Opt. Express **23**, A180–A191 (2015).
23. J.-S. Li, J.-X. Chen, L.-W. Lin, Z.-T. Li, Y. Tang, B.-H. Yu, and X.-R. Ding, "A detailed study on phosphor-converted light-emitting diodes with multi-phosphor configuration using the finite-difference time-domain and ray-tracing methods," IEEE J. Quantum Electron. **51**, 1–10 (2015).
24. H. Chen, K. Chen, C. Lin, C. Wang, C. Yeh, H. Tsai, M. Shih, and H. Kuo, "Improvement of lumen efficiency in white light-emitting diodes with air-gap embedded package," Microelectron. Reliab. **52**, 933–936 (2012).
25. K.-J. Chen, H.-C. Chen, M.-H. Shih, C.-H. Wang, H.-H. Tsai, S.-H. Chien, C. C. Lin, and H.-C. Kuo, "Enhanced luminous efficiency of WLEDs using a dual-layer structure of the remote phosphor package," J. Lightwave Technol. **31**, 1941–1945 (2013).